Higher level chromatic mechanisms for image segmentation

Thorsten Hansen　　　　　Department of Psychology, Justus-Liebig-University, Gieβen, Germany

Karl R. Gegenfurtner　　　　　Department of Psychology, Justus-Liebig-University, Gieβen, Germany

We used a noise-masking paradigm to investigate the number and properties of chromatic mechanisms involved in image segmentation. Observers were presented with a pattern of dynamic random squares, each independently modulated along a certain direction in DKL color space, either in the isoluminant plane or in the L − M luminance plane. A signal consisting of a rectangular region of squares, oriented horizontally or vertically, was added to the noise. The signal squares were spatially and temporally aligned to the noise squares, excluding the possibility of phase offsets to mediate segmentation performance. Noise and signal color directions were independently varied, and the signal contrast was measured at which an observer could reliably indicate the orientation of the signal. In a second set of experiments, the noise was simultaneously varying in two directions, symmetrically arranged around the signal direction. Masking was generally highest when signal and noise were modulated along the same direction and minimal for orthogonal noise. No difference was found between signals modulated along cardinal directions or intermediate directions. However, measured tuning widths critically depended on the type of noise: Noise modulated along one direction results in narrow tuning, whereas two-sided noise results in broad tuning. A chromatic detection model with multiple broadly tuned mechanisms successfully accounts for the experimental findings, both for narrow and broad tuning curves. Models with four broadly tuned cardinal mechanisms or multiple narrowly tuned mechanisms failed to reproduce the data. Our results suggest an important role for multiple, broadly tuned mechanisms in image segmentation.

Keywords: color vision, color mechanisms, noise masking, isoluminance

Introduction

Color vision starts with the absorption of light in three classes of cones. The cones have absorption spectra maxima at short (S), medium (M), and long (L) wavelengths. In the retinal ganglion cells, the signals from the cone photoreceptors are recombined to form two color-opponent channels: an L − M channel that is sensitive to signals modulated between a bluish green and reddish and an S − (L + M) channel that is sensitive to signals varying between yellow greenish and purple. Besides the two chromatic channels, there is an achromatic L + M luminance channel. The signals from the retina are then conveyed to the visual cortex via the lateral geniculate nucleus (LGN). Cells in the LGN have chromatic properties similar to those of retinal ganglion cells. Cells in the parvocellular layers of the LGN cluster into two groups of color-opponent cells, one preferring chromatic changes along the L − M direction and the other, preferably located in the koniocellular layers of the LGN, preferring changes along the S − (L + M) direction (Derrington, Krauskopf, & Lennie, 1984; Kaplan, Lee, & Shapley, 1990). Cells in the magnocellular layers of the LGN are mostly sensitive to luminance changes. These channels, defined anatomically and physiologically, correspond surprisingly well with the psychophysically defined *cardinal directions* of color space. Krauskopf, Williams,

and Heeley (1982) performed a habituation experiment where observers first habituated to a light modulated along one particular direction of color space. After 30 s, threshold was determined for lights modulated along the same or a different direction of color space. They found that habituation along one of three special directions in color space, which they called cardinal, led to threshold increases along the same cardinal direction but not along the other cardinal directions. For example, habituation to a color exchange along the L − M axis raised thresholds for subsequently viewed test lights with chromaticities at this axis. Thresholds for test lights lying on the orthogonal S − (L + M) axis remained the same as without previous habituation. Habituation in other directions, between the cardinal directions, led to unspecific threshold increases for all possible test lights. These results provided the empirical basis for color-opponent mechanisms in a low-level visual detection task (see also Pugh & Mollon, 1979, and Wandell & Pugh, 1980). Previous evidence for color-opponent mechanisms came from color naming or color cancellation, judgments presumably made at a relatively high level of the visual system and dependent on subjective criteria (Hering, 1878; Hurvich & Jameson, 1957).

The importance of cardinal directions was shown in numerous tasks. However, a reanalysis of the habituation data by Krauskopf, Williams, Mandler, and Brown (1986) showed that there might be more than three cardinal

mechanisms underlying psychophysical performance. Moreover, there is convincing evidence for the activity of a larger number of chromatic mechanisms in visual search (D'Zmura, 1991), color appearance (Webster & Mollon, 1991), chromatic detection in noise (Gegenfurtner & Kiper, 1992), and motion of chromatic plaid patterns (Krauskopf, Wu, & Farell, 1996). These results agree quite well with those from cortical physiology, where cells with a large variety of different color preferences were found in V1, V2, V3, and IT (Gegenfurtner, Kiper, & Levitt, 1997; Kiper, Fenstemaker, & Gegenfurtner, 1997; Komatsu, 1998, Komatsu, Ideura, Kaji, & Yamane, 1992; Lennie, Krauskopf, & Sclar, 1990; Wachtler, Sejnowski, & Albright, 2003). The chromatic tuning curves of cortical neurons typically cover a range of tuning widths. For example, tuning widths have been reported to vary from 10 to 90 deg in macaque V1 (Wachtler et al., 2003). In V2, Kiper et al. (1997) found a bimodal distribution of tuning curves, one clustering at approximately 30 deg and the other at approximately 60 deg (for a recent review, see Gegenfurtner, 2003).

Psychophysically, Gegenfurtner and Kiper (1992) used a noise-masking paradigm to measure the number and bandwidth of chromatic mechanisms. Observers had to detect a Gabor signal displayed in spatiotemporal chromatic noise. Signal and noise were independently and symmetrically modulated around a neutral gray point along lines in color space. Just like Krauskopf et al. (1982), Gegenfurtner and Kiper found that noise along one cardinal direction did not affect detection thresholds for signals along other cardinal directions. However, noise masking in intermediate directions led to specific threshold increases along the same intermediate direction of color space, whereas thresholds for the cardinal directions were unchanged. In other words, Gegenfurtner and Kiper found evidence for numerous chromatic mechanisms with a narrow bandwidth in color space.

It has been argued that narrow tuning can result from off-axis looking (D'Zmura & Knoblauch, 1998). When signal and noise can be separated by a linear plane, a mechanism that is less affected by the noise pattern can be used for the detection of the signal, a process known as off-axis looking. Off-axis looking results in artificially narrow tuning widths even if the underlying mechanisms have a broad tuning. To test whether the narrow tuning observed in the experiments described above may be due to off-axis looking, we used two-sided noise. For two-sided noise, the color of the noise pattern varies along two directions in color space, which are symmetrically spaced around the direction of the signal color, to minimize the possibility of off-axis looking.

Further chromatic detection experiments were performed by several other groups, but the results and interpretations varied considerably between the different laboratories, as detailed in the Discussion section.

We present experiments designed to resolve some of these issues, in particular, the number and tuning characteristics of chromatic mechanisms for image segmentation. We used spatially aligned signal and noise stimuli to test the idea that narrow tuning might be due to phase shifts between signal and noise. We also used one- and two-sided noises to determine the possible effects of off-axis looking. We found that measured tuning widths crucially depend on the type of noise: One-sided noise resulted in narrow tuning, whereas two-sided noise resulted in broad tuning curves. Psychophysical experiments are accompanied by a computational model of the chromatic detection performance. The model could account for both types of tuning curves obtained for the different noise types using multiple broadly tuned mechanisms. Other model variants, such as a model with broadly tuned mechanisms only along the cardinal directions or a model with multiple narrowly tuned mechanisms, could not account for the data. Overall, results suggest that chromatic detection is mediated by multiple broadly tuned mechanisms. The interactions between these multiple broadly tuned mechanisms lead to narrow or broad tuning curves, depending on the particular type of stimulus.

Methods

Observers were presented with a pattern of dynamic random squares, each of which was independently modulated along a certain direction in color space, either in the isoluminant plane or in a plane spanned by the luminance and $L - M$ chromatic mechanisms. A signal consisting of a rectangular region of squares, oriented horizontally or vertically, was added to the noise. The signal consisted of flickering squares modulated along one or two directions in color space. The signal squares were spatially and temporally aligned to the noise squares, excluding the possibility of phase offsets to mediate segmentation performance. Noise and signal color directions were independently varied, as was the contrast of the noise. For each signal and noise combination, the signal contrast was measured where an observer could reliably indicate the orientation of the signal rectangle.

Stimulus configuration

We used two setups to run the experiments. No difference in results between the two setups was found.

In the first setup, stimuli were displayed on a SONY Multiscan 20SE II color CRT monitor that was driven by a Cambridge Research VSG 2/4 graphics board at a refresh rate of 120 Hz noninterlaced. Observers were seated 114 cm away from the monitor, which extended 10×8 deg of visual angle. The images were generated on the monitor by reading through the picture memory in a raster scan and then interpreting the numbers in each location as a color defined in a 256-element color lookup table. Two 8-bit digital-to-analog converters, which were combined to produce an

intensity resolution of 14 bits, were used to control the intensity of each of the three monitor primaries. The luminances of each of the phosphors were measured at various output voltage levels using a Graseby Optronics Model 370 radiometer with a Model 265 photometric filter. A smooth function was used to interpolate between the measured points, and lookup tables were generated to linearize the relationship between output voltage and luminance. We also made sure that additivity of the three phosphors held over the range of intensities used in these experiments (Brainard, 1989). All the displays in the experiments of the first setup had a space- and time-averaged luminance of 26.0 cd/m^2.

In the second setup, stimuli were displayed on a SONY GDM F520 color CRT monitor that was driven by a Bits++ digital-to-analog converter, which provided an intensity resolution of 14 bits for each channel (Cambridge Research Systems, Cambridge, MA, USA). The refresh rate of the monitor was 60 Hz noninterlaced. The lookup tables for each of the three monitor primaries were generated with a resolution of 14 bits using an OptiCal photometer together with the calibration routines of Cambridge Research to linearize the relationship between output voltage and luminance. All the displays in the second setup had a space- and time-averaged luminance of 30.0 cd/m^2.

In both setups, a Photo Research PR 650 spectroradiometer was used to measure the spectra of the red, green, and blue phosphors at their maximum intensity setting. The spectra were multiplied with the CIE 1931 color matching functions, as revised by Judd (1951; see Table 1(5.5.2) in Wyszecki & Stiles, 1982), to derive CIE *x, y* chromaticity coordinates and the luminance *Y* of the phosphors (Irtel, 1992). All further references to luminance and photometric luminance refer to the $V(\lambda)$ curve as modified by Judd.

The primaries of our monitor had *x, y, Y* coordinates of 0.617, 0.346, 15.52 (red); 0.281, 0.604, 34.90 (green); and 0.153, 0.069, 4.223 (blue) in the first setup and 0.6172, 0.3473, 16.5393 (red); 0.2889, 0.6055, 35.0156 (green); and 0.1544, 0.0824, 4.6162 (blue) in the second setup. The monitor spectra were multiplied with the Smith and Pokorny (1975) cone fundamentals to calculate absorptions and contrasts in the L, M, and S cones.

Color space

Colors were chosen from a single plane in DKL color space, either in the isoluminant plane or in a plane spanned by the luminance and L − M chromatic mechanisms (Figure 1). The DKL color space (Derrington et al., 1984; Krauskopf et al., 1982) is based on the MacLeod and Boynton (1979) chromaticity diagram and is derived from cone contrast space, where color values are defined relative to a neutral gray point. The gray point had CIE *x, y, Y* coordinates as revised by Judd (1951) of 0.33, 0.35, 26 in the first setup and 0.33, 0.34, 30 in the second setup.
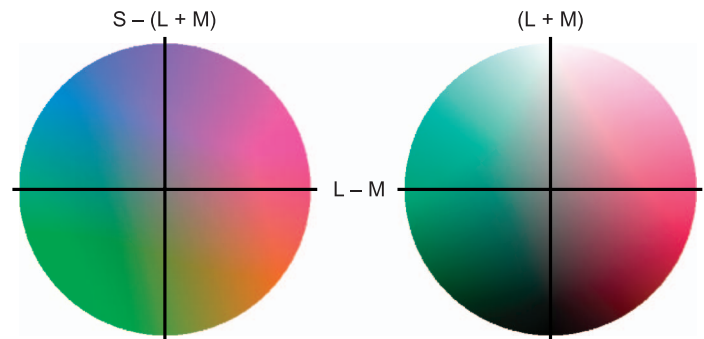

Figure 1. Color planes used in the experiments. Left: The isoluminant plane of the DKL color space. Right: A plane of the DKL color space spanned by the L − M and luminance mechanisms.

Two chromatic axes intersect at the gray point and span an isoluminant plane through the gray point. All lights in this plane have the same luminance as defined by the $V(\lambda)$ photopic luminosity function (Judd 1951; see Wyszecki & Stiles, 1982). Modulation along the (L − M) cone axis changes the excitations of the L and M wavelength-sensitive cones so that their sum (luminance) is kept constant and is invisible to the S wavelength-sensitive cones. Lights along this axis typically appear reddish and bluish green. Modulation along the S − (L + M) cone axis changes the excitation of S cones only and is invisible to L and M cones. Lights along this axis typically appear yellow greenish or purplish. The length of a vector that lies along a particular half-axis can be described in terms of the contrast delivered to the cone mechanisms (Smith & Pokorny, 1975). By modulating lights along the L − M axis, 9% contrast to the L cones and 17% to the M cones could be achieved. By modulating lights along the S − (L + M) axis, 83% contrast to the S cones could be achieved. Along the luminance axis, all three types of cones are equally modulated, up to values of 100% contrast.

Choice of color space and color space conversions

In the present study, we investigated higher order cortical color mechanisms. For the specification of the stimuli, we used the DKL color space because the DKL axes coincide with the preferences of LGN neurons, which provide the cortical input (Derrington et al., 1984). Like cone contrast space is the proper choice for experiments aimed at the characterization of *second-stage* postreceptoral mechanisms, DKL color space is the natural choice for investigating *higher order cortical* color mechanisms. Moreover, the DKL color space is motivated by both physiological (Derrington et al., 1984) and psychophysical (Krauskopf et al., 1982) findings. Finally, DKL color space is a linear transformation of cone contrast space. Overall, DKL color

space makes very few and well-motivated assumptions about the transformations of cone inputs.

In general, chromatic mechanisms are characterized by tuning curves drawn in a particular color space. A frequently raised issue is the (wrong) idea that the determined mechanisms somehow depend on the color space and that a change of color space will change the tuning widths of the mechanisms such that, for example, a linear broad tuning in DKL space results in a narrow tuning in cone contrast space, or vice versa. Intuitively, the argument seems to be correct in its straightforward way, which goes as follows: Consider a linear mechanism that has cosine tuning with regard to angle theta = arctan (y/x) in some space spanned by axes x and y. Scaling one axis x by a constant c leads to a new space with axes $x' = cx$ and y. Due to the nonlinear nature of arctan, the angles are different in the different color spaces, and the mechanism no longer has a cosine tuning. It is obviously correct that any scaling of the axes or a linear transformation in general can alter the shape of the curve. However, what obviously cannot be changed by this transformation is the nature of the underlying mechanism: A linear mechanism is a linear mechanism, independent of the space in which it is studied. What goes wrong in the above argument is that only the mechanism is transformed, not the lights that were used to stimulate the mechanism in the experiment. Scaling the axes also scales the lights that are no longer of equal amplitude in the newly rescaled color space. When stimulated by lights of a different amplitude, the linear mechanism will no longer show a cosine tuning. Using properly defined lights of equal amplitude in the new transformed color space would again nicely reveal the cosine tuning of the linear mechanisms. The same issue has been addressed more formally by Knoblauch and D'Zmura (2001), showing that the linear transformation of color space must be accompanied by a related but different transformation of the mechanisms in the dual space. Overall, "lights and neural responses do not depend on the color space used to represent the data" (Knoblauch & D'Zmura, 2001).

In this study, we present the experimental data and threshold curves in the same color space as we present the signal in the experiments, without any scaling of axes. This naturally ensures that for each data point in the color space where the data are presented and analyzed, the noise in the corresponding input stimuli has the same power. Because the noise power is the same in all directions, we can compare the threshold curves with cosine predictions. This point is critical for any study on chromatic mechanisms: A comparison with cosine predictions is valid only in a color space where the noise in the input stimuli has the same power in all chromatic directions. Any post hoc transformation of resulting threshold curves into another color space, which involves axes scaling (e.g., DKL to cone contrast space), violates the condition of equal noise power. In the present study, we ensured that the noise has the same power in all chromatic directions because we analyzed the results in the stimulus space, without any color space transformation or axis scaling.

Stimuli and paradigm

Observers were presented with a 16×16 pattern of dynamic random squares (noise), each square subtending 0.5 deg of visual angle. Each trial started with a blank gray screen shown for 500 ms, followed by the stimulus presentation of 10 frames of different noise patterns modulated at a frequency of 15 Hz, followed again by a blank screen for 500 ms. The noise squares were independently modulated along a certain direction in color space.

Two color distributions for the noise pattern were used. Colors of the noise pattern were uniformly distributed either along a single direction in color space (one-sided noise) or along two directions equally spaced around the direction of the signal color (two-sided noise). For two-sided noise, the color of the noise pattern varied along two directions in color space, which were symmetrically spaced around the direction of the signal color. At each frame, the noise value of a given square was drawn at random from one of the two noise vectors, independently across squares (see Figure 2).

A sample stimulus generated from signal and two-sided noise is shown in Figure 3.

The maximum chromatic contrast of the noise in all directions was 0.5 for one-sided noise in the isoluminant plane, 0.4 for one-sided noise in the L − M luminance plane, and 0.25 for two-sided noise. The maximal available contrast in the DKL space was defined to be 1.0. The signal, which was added to the noise, consisted of 12×3 squares, oriented horizontally or vertically. The signal consisted of flickering squares modulated along one direction of color space. The signal squares were spatially and temporally aligned to the noise squares, excluding the possibility of phase offsets to mediate segmentation performance (Figure 4). Sample stimuli for the two noise types in the two color
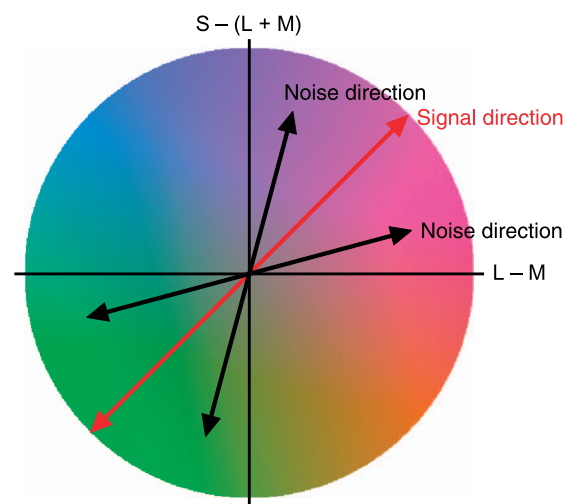

Figure 2. Two-sided noise. For two-sided noise, the noise pattern is modulated along two directions that are symmetrically spaced around the signal direction.
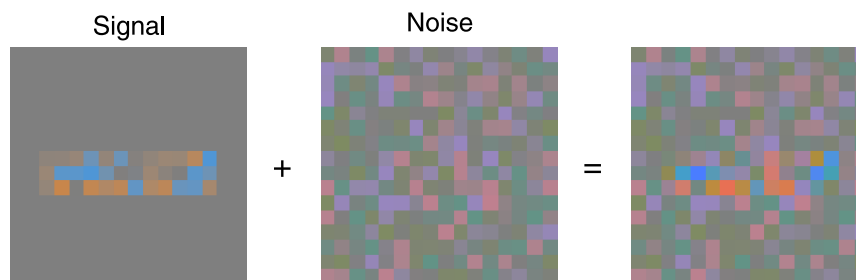
Figure 3. Sample stimulus generated from signal and two-sided noise. The direction of the signal color is 135 deg; the noise has a 45-deg offset at either side of the signal direction and is modulated along 90 and 180 deg.

planes are provided as Supplementary Material [one-sided noise: isoluminant plane (movie1.mov), L − M luminance plane (movie2.mov); two-sided noise: isoluminant plane (movie3.mov), L − M luminance plane (movie4.mov)]. Noise and signal color directions were independently varied, as was the contrast of the noise. For each signal and noise combination, the signal contrast was measured at which an observer could reliably indicate the orientation of the signal rectangle.

Interleaved staircases were used to determine thresholds for detecting the signal.

Tuning curves were determined for the cardinal directions 0 and 90 deg and for various intermediate directions, as detailed in the next paragraph. The intermediate directions were defined in a single unscaled DKL color space and were the same for all observers. Because the intermediate directions were defined in the stimulus space, they did not necessarily reflect the optimal stimuli for mechanisms tuned to intermediate directions.

To measure detection at a particular chromatic direction, we kept the direction of the noise fixed and varied the

direction of the signal relative to the noise. This procedure was employed for the experiments using one-sided noise. For two-sided noise, one cannot use this procedure because the noise varies along two directions. We thus used an alternative procedure where we kept the direction of the signal fixed and varied the noise.

For the experiments using one-sided noise, tuning curves were determined for six test directions of 0, 30, 60, 90, 120, and 150 deg. For each test direction, eight directions of the signal were tested, with chromatic directions relative to the test directions of −60, −30, −15, 0, 15, 30, 60, and 90 deg.

For two-sided noise, tuning curves were determined for four test directions of 0, 45, 90, and 135 deg. For each test direction, seven directions of the noise were tested, with chromatic directions relative to the test directions of 0, 15, 30, 45, 60, 75, and 90 deg. Thus, for both noise types, the nearest sampling of the direction relative to the test direction was always 15 deg.

The experiments with one-sided noise were replicated with fixed signal directions and varying noise direction to
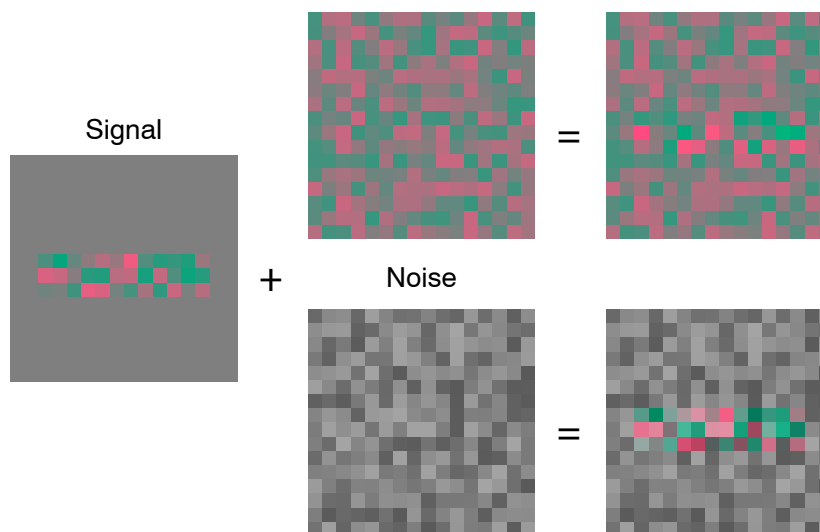

Figure 4. Masking paradigm. A sample rectangular signal with a chromatic modulation along the L − M axis is added to noise modulated either along the same axis or along an orthogonal axis (luminance) in DKL space. When signal and noise are modulated along the same axis, detection is hardest and threshold is maximal. On the contrary, when signal and noise are modulated along orthogonal directions, the detection is almost as easy as without noise, resulting in almost no increase in threshold as compared with the detection without noise.

control for the effect of varying the signal versus varying the noise. The measured threshold curves were unaffected by the particular presentation of the stimuli, as detailed in the Results section.

A simple up–down method (Levitt, 1971) was used to adjust the signal amplitude to threshold. After three positive responses in a row, the signal magnitude was decreased by 0.1 log units; after each negative response, it was increased by the same amount. After six reversals, a staircase was terminated. Psychometric functions were then fitted using the psignifit toolbox for Matlab (Version 2.5.41, see http://bootstrap-software.org/psignifit/), which implements the maximum likelihood method described by Wichmann and Hill (2001).

Observers

One of the authors (TH) and six naive observers (BL, CH, JB, LL, KH, and KL) with normal color vision and normal or corrected-to-normal visual acuity participated in this study. There was no systematic difference in results between the different observers. Each experimental condition was run by three observers. Due to the limited availability of observers, not all experiments were run by all observers.

Results

The noise-masking paradigm: Basic results

Masking noise leads to a linear increase in threshold contrast (Legge, Kersten, & Burgess, 1987; Pelli, 1981). Gegenfurtner and Kiper (1992) showed that this holds for

stimuli along the L − M isoluminant color direction as well. Furthermore, when signal and noise lie on different cardinal directions, the noise has no masking effect on the signal. A replication of this result for our paradigm is shown in Figure 5.

This fact can be used to systematically measure the tuning of chromatic mechanisms in any plane of color space, as has been done by a number of researchers using different stimuli (D'Zmura & Knoblauch, 1998; Gegenfurtner & Kiper, 1992; Giulianini & Eskew, 1998; Goda & Fujii, 2001; Li & Lennie, 1997; Sankeralli & Mullen, 1997; Stromeyer, Thabet, Chaparro, & Kronauer, 1999).

In the present study, we used this paradigm to investigate the tuning widths of chromatic mechanisms in the isoluminant and the L − M luminance plane using two types of noise patterns. In the first set of experiments, we used one-sided noise; in the second, two-sided noise. For each combination of noise types (either one- or two-sided) and color planes (either isoluminant or L − M luminance) studied, we show three figures: (1) representative data of a single observer; (2) data averaged across three observers; and (3) data averaged across chromatic directions for the same three observers, as in (2).

One-sided noise

For the experiments using one-sided noise, the direction of the noise was fixed and defined the test direction, whereas the direction of the signal relative to the noise was varied. Tuning curves in the isoluminant plane were determined for six test directions of 0, 30, 60, 90, 120, and 150 deg. Tuning curves in the L − M luminance plane were determined for four test directions of 0, 45, 90, and 135 deg. For each test direction, eight directions of the signal were tested, with
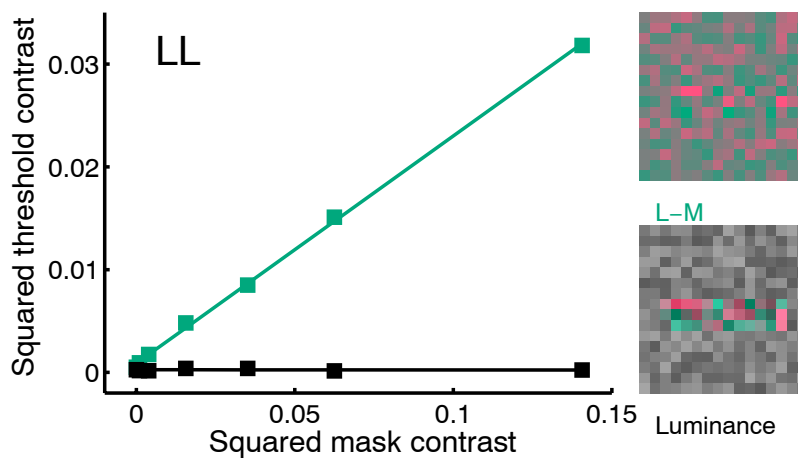

Figure 5. Results of noise masking. Masking noise leads to a linear increase in threshold when signal and noise are modulated along the same chromatic direction in color space (green line). When signal and noise are modulated along orthogonal directions in color space, for example, along the luminance and L − M direction, respectively, the noise has no masking effect on the signal (black line). Data are averaged across three repetitions of the experiment for observer LL. Error bars are smaller than the symbol size.

chromatic directions relative to the test directions of −60, −30, −15, 0, 15, 30, 60, and 90 deg. Because signal and noise were both symmetric modulations around the neutral gray point, measurements were made in only one of two opposing directions. For each data point, the *direction* from the origin indicates the chromatic direction of the signal and the *distance* from the origin indicates the detection threshold for the particular combination of signal and noise direction. The small central gray curve indicates detection threshold in the absence of noise.

Tuning in the isoluminant plane, one-sided noise

In the first experiment, tuning widths in the isoluminant plane were determined using one-sided noise. Results at six test directions (0, 30, 60, 90, 120, and 150 deg) for a single observer are shown in Figure 6.

For each of the six chromatic directions of the noise tested, the threshold curves were remarkably consistent. In particular, no difference between noise modulated at cardinal directions and that at noncardinal directions was found. In almost all cases, thresholds were highest when signal and noise were modulated along the same direction and rapidly declined with increasing separation in color direction between signal and noise. In particular, when signal and noise were modulated along orthogonal directions, the thresholds were similar to those obtained in the absence of noise. This holds true for any signal direction, both along the cardinal axes and along the intermediate axes. Here and in the following, we use the term *orthogonal* with respect to the particular data representation used, without claiming any fundamental status of such orthogonality.

We also determined tuning curves in the isoluminant plane averaged across three observers (Figure 7). Averaged data show no systematic difference to the data obtained for a single observer. Tuning curves were narrow, and thresholds for orthogonal noise were similar to those obtained without noise. For test directions of 120 and 150 deg (bottom row in Figure 7), orthogonal noise led to a small increase in threshold. The reason for this is unclear but may be due to cross-talk between mechanisms.

Next, we determined the average tuning width of the chromatic mechanisms. The tuning width is important because it can be related to the stage of color processing involved in the particular task. Second-order cone-opponent channels are characterized by broad cosine tuning curves with a half-width at half-height (HWHH) of 60 deg. Cosine tuning curves result from a linear combination of cone signals. Chromatic channels at higher stages that *linearly* combine cone-opponent signals also have a broad tuning of 60 deg. A bandwidth narrower than 60 deg is typically interpreted to result from a *nonlinear* combination of cone-opponent signals, involving higher order mechanisms (e.g., Clifford, Spehar, Solomon, Martin, & Zaidi, 2003; De Valois & De Valois, 1993; D'Zmura & Lennie, 1986; Gegenfurtner
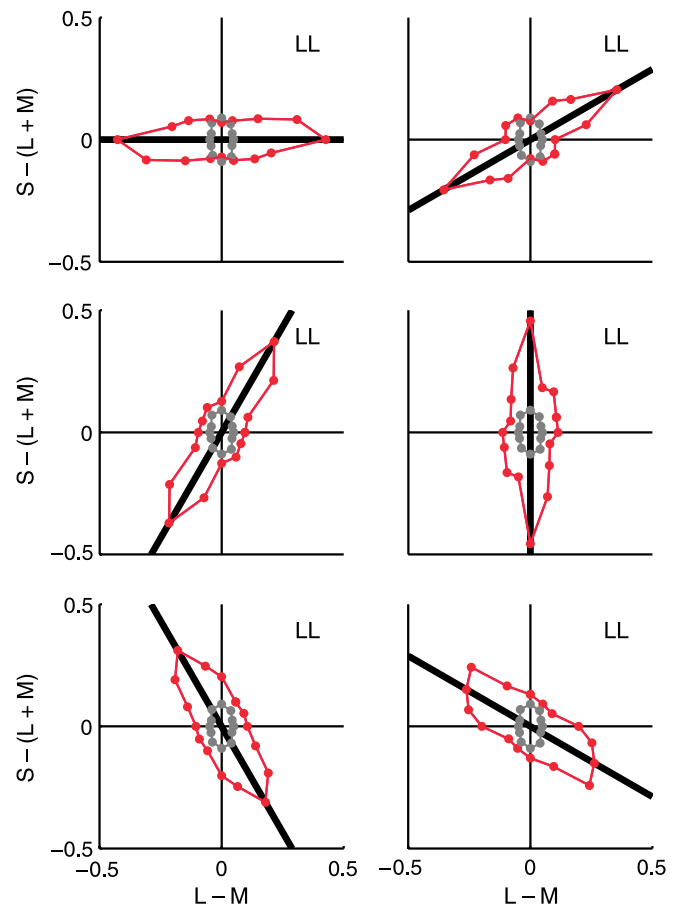

Figure 6. Narrow tuning curves observed for one-sided noise in the isoluminant plane for a single observer (LL). Six test directions were used, having color azimuths of 0, 30, 60, 90, 120, and 150 deg (indicated by the bold black line). The small gray curve in the center indicates detection thresholds in the absence of noise. For each chromatic direction of the noise, the threshold curves peak at the chromatic direction of the noise and have a narrow tuning. Signals modulated along orthogonal directions have almost no effect on the detection threshold, as indicated by the points lying close to the central gray curve.

& Kiper, 1992; Goda & Fujii, 2001; Webster & Mollon, 1994; Zaidi & Shapiro, 1993).

To determine the average tuning width, we aligned the different chromatic directions of the noise at 0 deg and plotted the averaged threshold curves with respect to the difference between signal and noise. Data averaged across three observers are shown in Figure 8. The average tuning has an HWHH that is considerably narrower than predicted by a linear mechanism.

Tuning in the L − M luminance plane, one-sided noise

In the second experiment, we replicated our first experiment in the L − M luminance plane. Results at four test directions (0, 45, 90, and 135 deg) for a single observer are
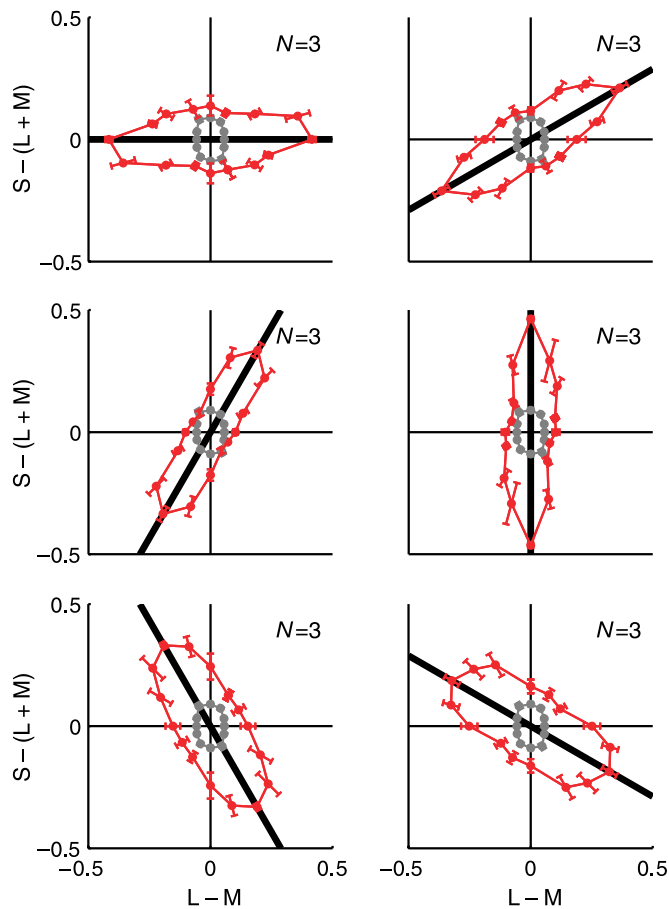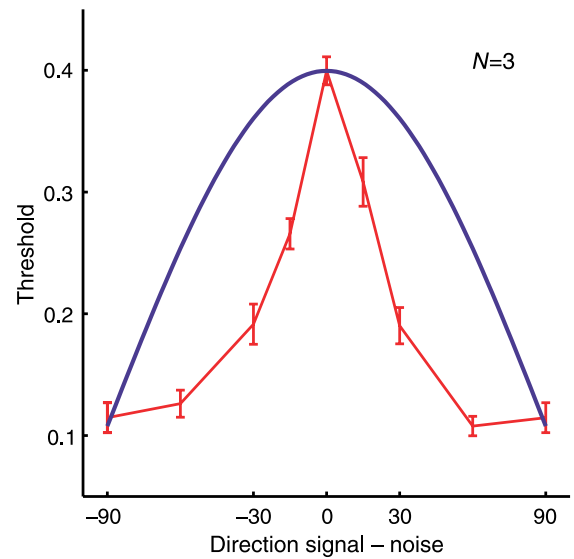
Figure 8. Average tuning in the isoluminant plane for three observers (BL, LL, and KL). Error bars denote standard error. Tuning width is considerably narrower than a prediction by a cosine tuning function (blue curve), resulting from a linear combination of cone inputs.

colors at 0 deg. Data averaged across three observers are shown in Figure 11. Similar to tuning in the isoluminant plane, the average tuning has an HWHH that is considerably narrower than predicted by a linear mechanism.

Variation of the signal versus variation of the noise

In the experiments with one-sided noise shown so far, the threshold curves for a given chromatic direction were obtained by fixing the noise direction at the particular chromatic direction and varying the direction of the signal. Alternatively, one can also vary the chromatic direction of the noise while holding the chromatic direction of the signal constant. To test whether these different variations may affect the obtained threshold curves, we replicated the above experiments in both chromatic planes (isoluminant and L − M luminance) with a fixed signal and varying noise.

Data for the isoluminant plane are shown in Figure 12 and those for the L − M luminance plane are shown in Figure 13. In almost all cases, no significant difference between the two methods occurred. The only exception is for one observer (CH) in the isoluminant plane (Figure 12) when signal and noise were varied along the same direction (0 deg). This effect was not stable across observers and did not occur for the same observer (CH) in the L − M luminance plane. Overall, both methods of varying the signal versus varying the noise give the same results. This argues against any cognitive effect of attention or strategy where one might expect a lower threshold if the direction of the signal to be detected is kept fixed,
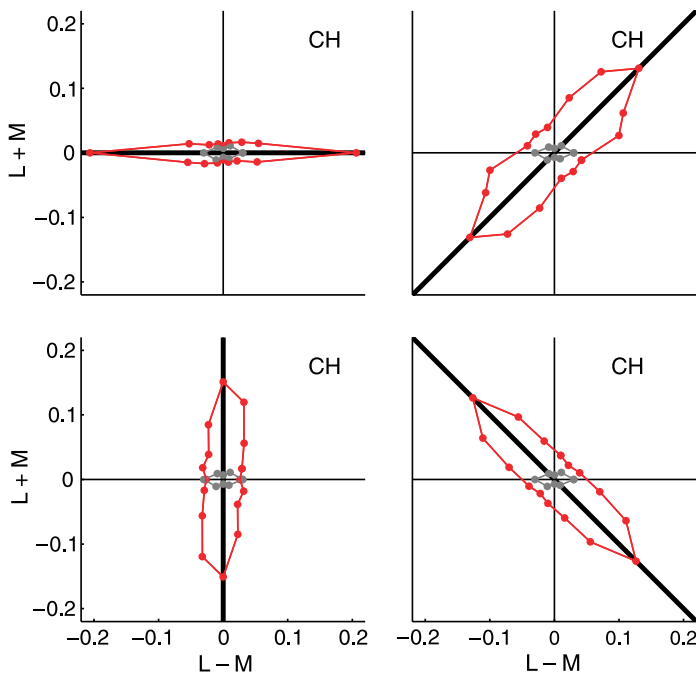
Figure 7. Narrow tuning curves observed for one-sided noise in the isoluminant plane, data averaged across three observers (BL, LL, and KL). Error bars denote standard error. Six test directions were used, having color azimuths of 0, 30, 60, 90, 120, and 150 deg (indicated by the bold black line). The small gray curve in the center indicates detection thresholds in the absence of noise, averaged across the three observers. For each chromatic direction of the noise, the threshold curves peak at the chromatic direction of the noise and have a narrow tuning. Signals modulated along orthogonal directions have almost no effect on the detection threshold, as indicated by the points lying close to the central gray curve.

shown in Figure 9. The results are essentially the same as obtained in the isoluminant plane: Thresholds are highest when signal and noise are modulated along the same direction and rapidly decline with increasing difference between signal and noise direction.

We also determined tuning curves in the L − M luminance plane averaged across three observers (Figure 10). Again, averaged data showed no systematic difference in the data obtained for a single observer. Tuning curves were narrow, and thresholds for orthogonal noise were similar to those obtained without noise. Furthermore, no difference between cardinal and noncardinal directions was found.

Furthermore, as in the isoluminant plane, the average tuning width was determined by aligning the different signal

Figure 9. Narrow tuning curves observed for one-sided noise in the L − M luminance plane for a single observer (CH). Four signal colors are used, having color azimuths of 0, 45, 90, and 135 deg (indicated by the bold black line). The small central gray curve indicates detection thresholds in the absence of noise. For each chromatic direction of the noise, the threshold curves peak at the chromatic direction of the noise and have a narrow tuning. Signals modulated along orthogonal directions have almost no effect on the detection threshold, as indicated by the points lying close to the central gray curve.

Figure 10. Narrow tuning curves observed for one-sided noise in the L − M luminance plane, data averaged across three observers (CH, JB, and KH). Error bars denote standard error. Four signal colors are used, having color azimuths of 0, 45, 90, and 135 deg (indicated by the bold black line). The small central gray curve indicates detection thresholds in the absence of noise, averaged across the three observers. For each chromatic direction of the noise, the threshold curves peak at the chromatic direction of the noise and have a narrow tuning. Signals modulated along orthogonal directions have almost no effect on the detection threshold, as indicated by the points lying close to the central gray curve.

allowing an observer to focus attention on this signal. Rather, it is more likely that the narrow tuning observed is due to off-axis looking, as discussed in the next section. Off-axis looking is not a deliberate decision of the observer, but an automatic process at the first stages of visual processing.

Overall, the data show that the measured threshold curves were unaffected by the particular presentation of the stimuli (i.e., whether noise or signal direction was kept constant during a block of presentations).

Two-sided noise

We used two-sided noise to determine the possible effects of off-axis looking. For two-sided noise, the direction of the signal was kept fixed and defined the test direction, whereas the direction of the noise relative to the signal was varied. Tuning curves were determined for four test directions of 0, 45, 90, and 135 deg. For each test direction, seven directions of the noise were tested, with chromatic directions relative to the test directions of 0, 15, 30, 45, 60, 75, and 90 deg.
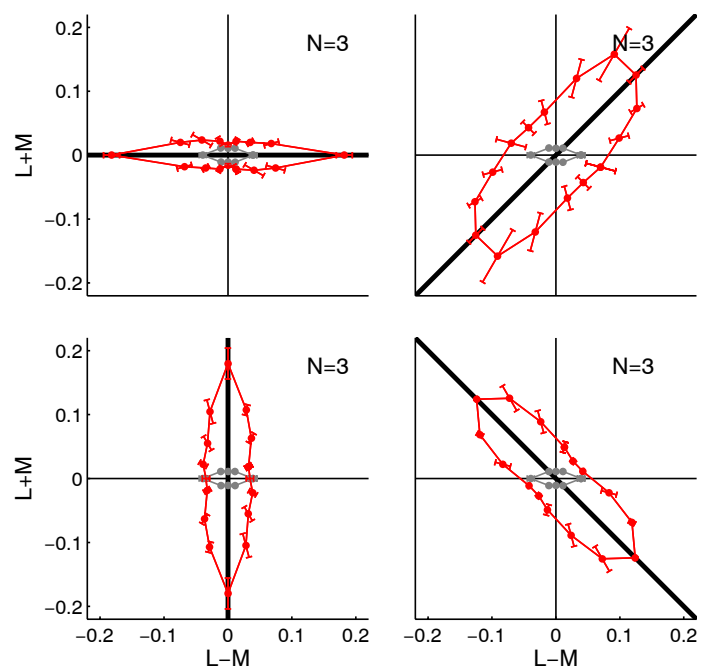
Tuning in the isoluminant plane, two-sided noise

In the first experiment using two-sided noise, tuning widths in the isoluminant plane were determined. Results for a single observer are shown in Figure 14. Thresholds were highest when the noise was modulated along directions close to the signal direction. Unlike the data for one-sided noise, we found not always a pronounced peak in the threshold curves when signal and noise directions coincided rather than a broader range of noise directions (up to ±45 deg relative to the signal direction) that resulted in high thresholds of similar magnitude. In one case (90-deg signal, lower left panels in Figures 14 and 15), there was a dip in the threshold curves when signal and noise coincided, resulting in a bow-tie-shaped tuning curve. Similar to the results obtained for one-sided noise, orthogonal noise had almost no effect. Overall, the tuning widths for two-sided noise are broader as compared with the results obtained with one-sided noise.

Note that because we kept the direction of the signal fixed, the threshold curves in the absence of noise (gray circles in Figures 14 and 15 and in Figures 17 and 18 for the L − M luminance plane) are now circles with a radius defined by the detection threshold for this particular signal direction.
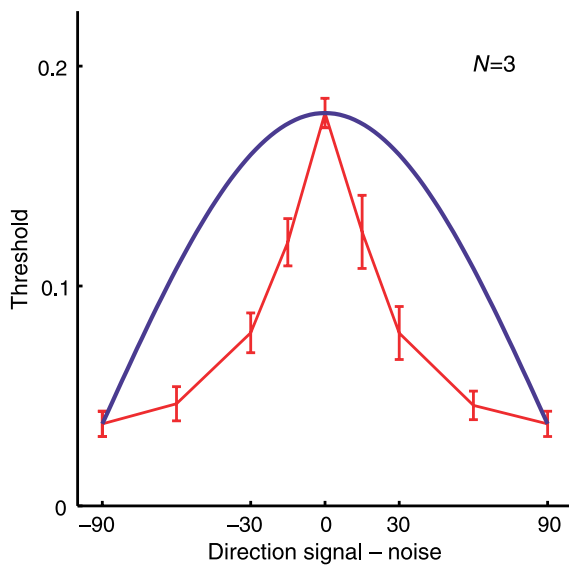
Figure 11. Average tuning in the L − M luminance plane for three observers (CH, JB, and KH). Error bars denote standard error. Tuning width is considerably narrower than a prediction by a cosine tuning function (blue curve), resulting from a linear combination of cone inputs.

Next, we determined tuning curves in the isoluminant plane averaged across three observers (Figure 15). Similar to the curves for a single observer, we found broad tuning and almost no increase in threshold for orthogonal noise for all signal directions.

Finally, we determined the average tuning width averaged across all chromatic directions for the three observers. Because positive and negative offsets between signal and noise define the same stimulus for the two-sided noise condition, only positive offsets were plotted. Data averaged across three observes are shown in Figure 16. Contrary to the results obtained for one-sided noise, the average tuning was broad and followed a cosine function, consistent with a linear combination of cone inputs. When signal and noise directions coincided (0 deg), there was a small dip in the averaged tuning curve. The reason for this dip is unclear. Preliminary simulation studies suggest that it may be related to a variation of the peak chromaticities of the detection mechanisms. In the simulations, a smaller variation along the chromatic direction of the signal to be detected leads to the observed dip in the detection threshold curve.

Tuning in the L − M luminance plane, two-sided noise

In the final experiment, tuning widths in the L − M luminance plane were determined using two-sided noise. Results at four signal directions for a single observer are shown in Figure 17. Similar to the results obtained for two-sided noise in the isoluminant plane, thresholds were highest when the noise was modulated along directions close to the signal direction. In one case (0-deg signal,
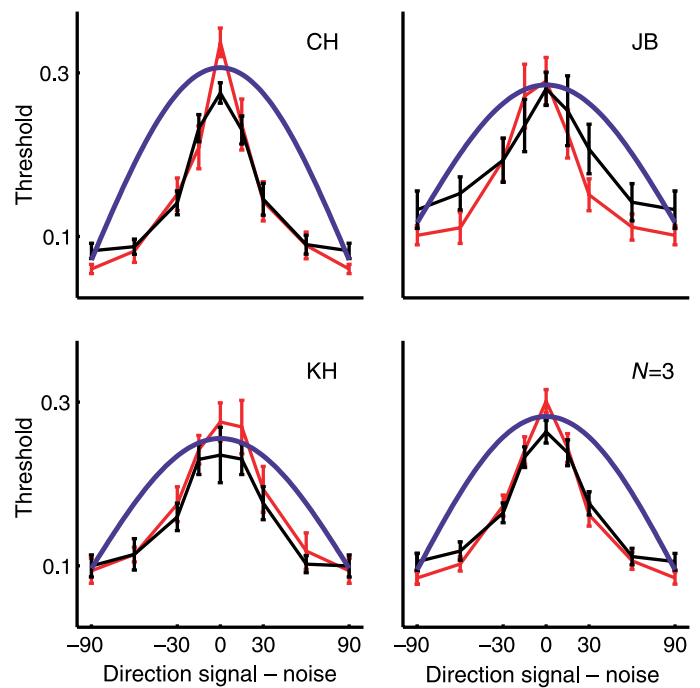

Figure 12. Variation of the signal (red) as compared with variations of the noise (black) in the isoluminant plane has almost no effect on average tuning curves. Data are shown for three observers (panels labeled CH, JB, and KH) and averaged across these three observers (bottom right panel labeled "N = 3"). Error bars denote standard error. Red curves denote tuning curves for varying the signal while keeping the noise fixed; black curves, tuning curves for keeping the signal fixed and varying the noise. Almost no significant difference in the average tuning curves between both methods was found.

upper left panels in Figures 17 and 18), there was a dip in the threshold curves when signal and noise coincided, resulting in a bow-tie-shaped tuning curve.

Next, we determined tuning curves in the L − M luminance plane averaged over three observers (Figure 18). Similar to the results obtained for a single observer, the thresholds were highest when the noise was modulated along directions close to the signal direction. When the signal was modulated along the cardinal directions (Figures 17 and 18, left column), we found no increase in threshold for orthogonal noise. However, for the intermediate signal directions tested, a small increase in threshold occurred, presumably as an effect of the higher sensitivity to luminance variations.

Finally, we determined the average tuning width averaged across all chromatic directions for the three observers. Similar to the results obtained for the two-sided noise in the isoluminant plane, the averaged tuning curve was broad, as predicted by a linear combination of cone inputs (Figure 19). Similar to the results obtained in the isoluminant plane, the bow-tie-shaped threshold curves resulted in a small dip at 0 deg in the averaged curve when signal and noise coincided. As stated above for the results in the isoluminant plane, the dip may be caused by a decrease of the variation of the
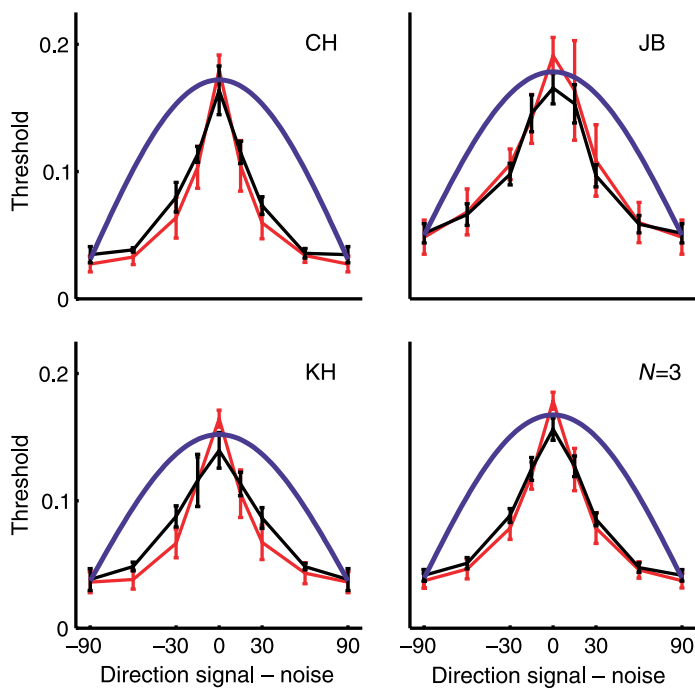
Figure 13. Variation of the signal (red) as compared with variations of the noise (black) in the L − M luminance plane has almost no effect on average tuning curves. Data are shown for three observers (panels labeled CH, JB, and KH) and averaged across these three observers (bottom right panel labeled "$N = 3$"). Error bars denote standard error. Red curves denote tuning curves for varying the signal while keeping the noise fixed; black curves, tuning curves for keeping the signal fixed and varying the noise. No significant difference in the average tuning curves between both methods was found.
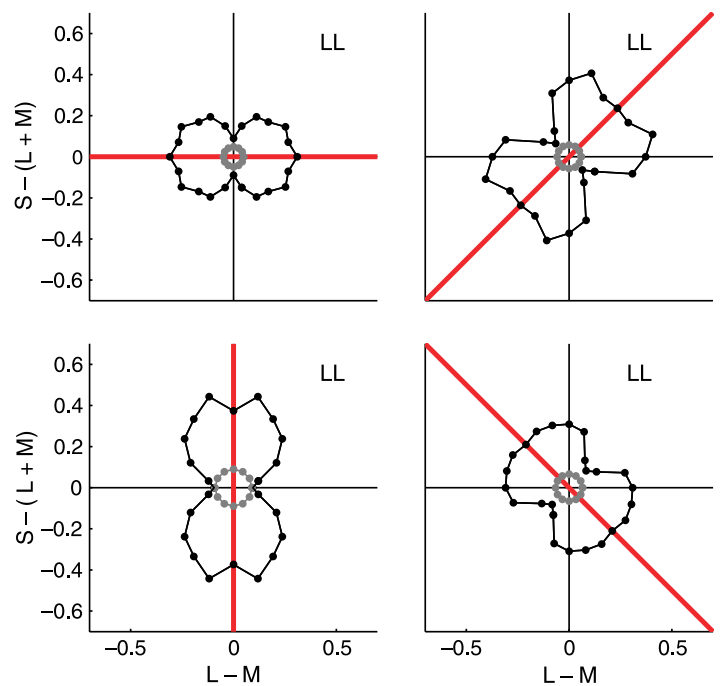
Figure 14. Broad tuning curves observed for two-sided noise in the isoluminant plane for a single observer (LL). Four signal colors are used, having color azimuths of 0, 45, 90, and 135 deg (indicated by the bold red line). The small gray circle indicates detection thresholds in the absence of noise. For each signal color, the threshold curves peak at the signal color and have a broad tuning. For all signal colors, noise along orthogonal directions has almost no effect on the detection threshold, as indicated by the points lying on the small central gray circle.

peak chromaticities along the chromatic direction of the signal to be detected.

Overall, the results of the detection experiments using different types of noise can be summarized as follows: Narrow tuning is observed for one-sided noise, whereas broad linear tuning is observed for two-sided noise. The cardinal directions play no specific role in this task: For any signal direction, whether cardinal or intermediate, threshold is maximal when the noise is modulated along directions close to the signal direction and shows no increase for orthogonal noise. Results hold true for the isoluminant and the L − M luminance plane.

Simulations

The chromatic detection experiments presented in the previous section show that the tuning width of chromatic detection is stimulus dependent. For one-sided noise, chromatic tuning was narrower than linear, with an average HWHH of 25.5 deg, whereas for two-sided noise, chromatic tuning was perfectly predictable by a linear combination of cone inputs, resulting in a cosine tuning curve (HWHH of 60 deg).

The results allow for a number of different interpretations regarding the number and nature of the underlying chromatic detection mechanisms. For example, one could assume that the different stimuli are detected at different stages that have chromatic detection mechanisms with either narrow or broad tuning widths. Instead, one could assume that the same broadly tuned mechanisms are involved in the detection of both kinds of stimuli and that the different tuning widths observed result from off-axis looking.

Chromatic detection model

To further investigate the number and nature of the underlying detection mechanisms, we used a chromatic detection model to simulate the observers' response characteristics. The goal of this model study was not to derive the best fit to the data but to investigate whether the different tuning curves can be accounted for by the same underlying circuit. In particular, we were interested in the generation of narrow tuning curves due to off-axis looking.

We used a line-element model that has been successfully employed to model discrimination tasks in a number of different domains, such as wavelength (von Helmholtz,
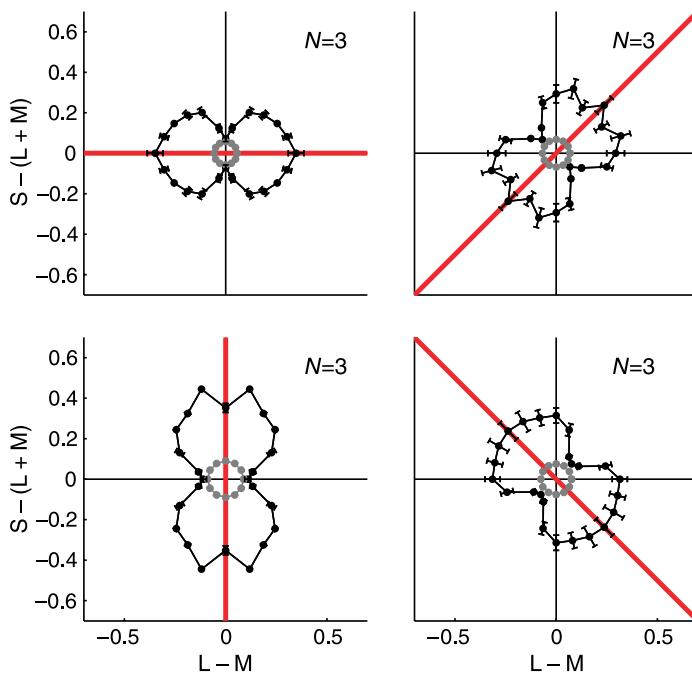
Figure 15. Broad tuning curves observed for two-sided noise in the isoluminant plane, data averaged across three observers (CH, LL, and JB). Error bars denote standard error of the mean. Four signal colors are used, having color azimuths of 0, 45, 90, and 135 deg (indicated by the bold red line). The small central gray circle indicates detection thresholds in the absence of noise, averaged across the three observers. For each signal color, the threshold curves peak at the signal color and have a broad tuning. For all signal colors, noise along orthogonal directions has almost no effect on the detection threshold, as indicated by the points lying on the small central gray circle.

1867/1924), spatial frequency (Wilson & Gelb, 1984), and global motion (Watamaniuk, Sekuler, & Williams, 1989). More recently, Goda and Fujii (2001) proposed a similar model to analyze the discrimination of multicolored textures.

The chromatic line-element model comprises two main processing stages. At the first stage, color signals are processed by multiple channels each tuned to a particular direction in color space. The number N of channels and their tuning width k are the basic model parameters. Because we did not fit the N channels to the data, the model had only two free parameters, N and k, independent of the number of channels used. This allowed us to compare the outcome of different models without the need to compensate for the different numbers of channels used by the different models.

At the second stage, the difference in channel responses to the background and a signal region of either horizontal or vertical orientation is determined. The larger difference determines the model estimate of the signal orientation. Given an input stimulus, the model thus responds with the estimated orientation of the signal. Model responses for signals of varying contrasts are determined, each presented in 1,000 trials with different realizations of the noise process.
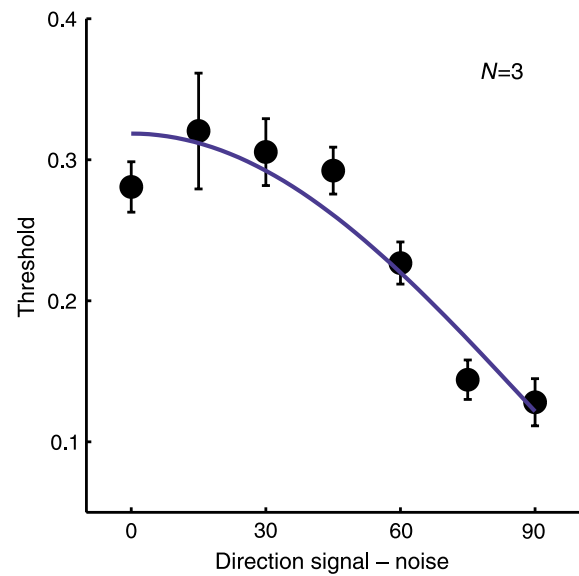

Figure 16. Average tuning in the isoluminant plane for three observers (CH, LL, and JB). Error bars denote standard error. Tuning width is consistent with a prediction by a cosine tuning function (blue curve), resulting from a linear combination of cone inputs.

Psychometric functions are then fitted to the model responses for different contrast levels of the signal using the psignifit toolbox for Matlab (Version 2.5.41, see http://bootstrap-software.org/psignifit/), which implements the maximum likelihood method described by Wichmann and Hill (2001). In the following, we describe the two main processing stages of the model in more detail.

The core components of the model are chromatic detection mechanisms sensitive to second-order cone-opponent features. The model has a number of mechanisms N that are defined in a single plane of the cone-opponent DKL color space. Each mechanism has the same raised cosine-shaped tuning profile but different peak sensitivities. Formally, the sensitivity profile S of a mechanism with peak sensitivity μ sensitive to different color azimuths θ is given by

$$S_i(\theta) = \left[\cos^k(\theta - \mu)\right]^+, \qquad \mu = 306 \deg \frac{i}{N} + \eta.$$

The operator $[x]^+ = \max(x, 0)$ denotes half-wave rectification, and the parameter k determines the tuning width of the sensitivity profile (D'Zmura & Knoblauch, 1998). A value of $k = 1$ results in the standard cosine profile, consistent with a linear combination of the cone-opponent signal. Increasing k sharpens the profile. Sensitivity profiles for different values of k are shown in Figure 20. The sensitivity functions are normalized such that they integrate to unity.

The parameter μ determines the peak sensitivity of the N chromatic channels, which are equally spaced in the chromatic plane. For example, $N = 4$ mechanisms would
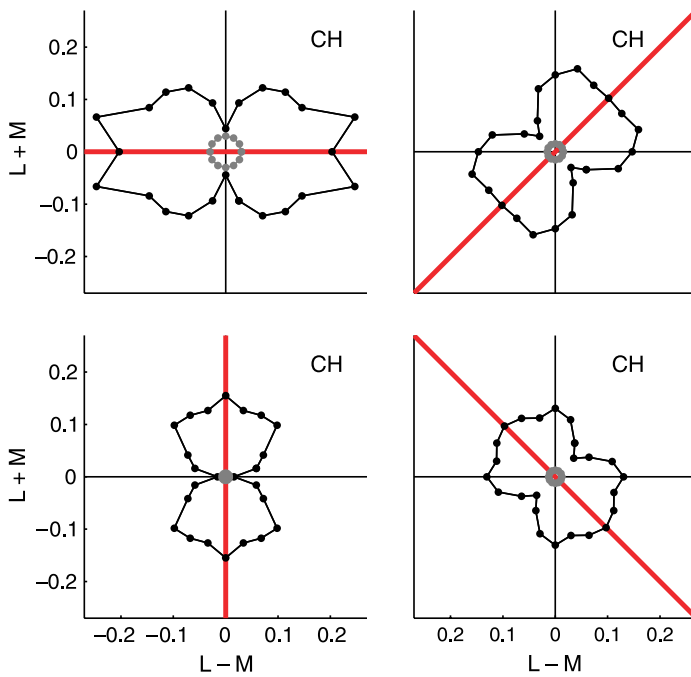
Figure 17. Broad tuning curves observed for two-sided noise in the L − M luminance plane for a single observer (CH). Four signal colors are used, having color azimuths of 0, 45, 90, and 135 deg (indicated by the bold red line). The small central gray circle indicates detection thresholds in the absence of noise. For each signal color, the threshold curves peak at the signal color and have a broad tuning. For all signal colors, noise along orthogonal directions has almost no effect on the detection threshold, as indicated by the points lying close to the small central gray circle.

Figure 18. Broad tuning observed for two-sided noise in the L − M luminance plane, data averaged across three observers (CH, JB, and TH). Error bars denote standard error. Four signal colors are used, having color azimuths of 0, 45, 90, and 135 deg (indicated by the bold red line). The small central gray curve indicates detection thresholds in the absence of noise, averaged across the three observers. For each signal color, the threshold curves peak at the signal color and have a broad tuning. For all signal colors, noise along orthogonal directions has almost no effect on the detection threshold, as indicated by the points lying close to the small central gray curve.

result in a spacing of 360/4 = 90 deg; $N = 5$ mechanisms in a spacing of 360/5 = 72 deg; $N = 8$ mechanisms in a spacing of 360/8 = 45 deg; and so on. Simulations are confined to a single plane in color space, with mechanisms extending from the origin in a particular direction. Thus, a model with $N = 4$ cardinal mechanisms has two mechanisms along each cardinal axis in a single plane of color space, e.g., +(L − M), −(L − M), +[S − (L + M)], −[S − (L + M)], with corresponding chromatic directions of 0, 180, 90, and 270 deg).

Extending the model by Goda and Fujii (2001), the peak sensitivities are allowed to vary at each stimulus position by a normally distributed noise process η with a standard deviation of 10 deg to model the variability of the preferred hue in individual LGN neurons as observed experimentally (Derrington et al., 1984). At the start of the simulations, the peak sensitivities were randomly jittered as described above at each of the 16 × 16 stimulus positions; they were then kept fixed at these chromatic directions during the whole simulated experiment. This procedure was used for each of the model types studied. Running the simulations with setting $\eta = 0$ (i.e., allowing no variability) would result in tuning curves with artificial dips at those chromatic
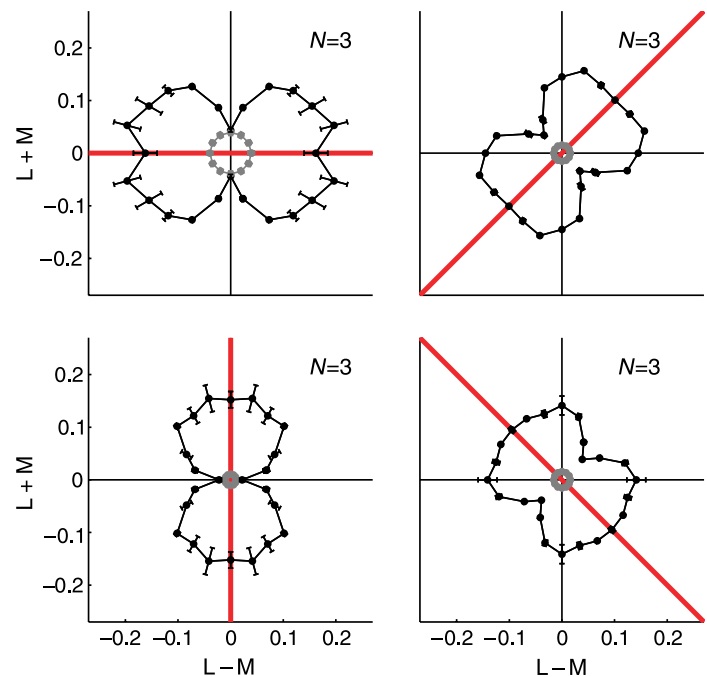
directions where the peak sensitivities μ and the noise direction coincide. Figure 21 visualizes the variation of the peak sensitivities for a model with $N = 4$ mechanisms.

The number N of mechanisms and the tuning width of the sensitivity profile as determined by k are the basic model parameters. For example, a standard quasi-linear model with four broadly tuned mechanisms along the cardinal axes is specified by $N = 4$, $k = 1$.

Each channel i integrates color signals within a particular region A of the stimulus, resulting in an average response $R_{A,i}$ of channel i to the stimulus covering region A

$$R_{A,i} = \frac{1}{\|A\|} \sum_{(x,y) \in A} r(x,y) S_i[\theta(x,y)],$$

where r is the chromatic contrast and θ is the chromatic direction of the square at the particular position (x, y); $\|A\|$ denotes the magnitude of the set A (i.e., the number of elements in A).
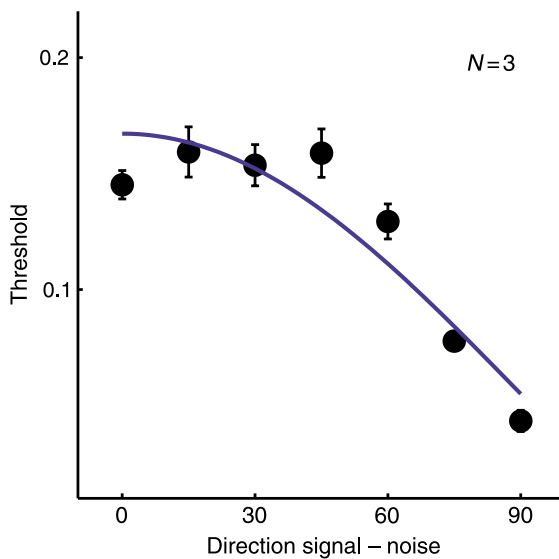
Figure 19. Average tuning in the L − M luminance plane for three observers (CH, JB, and TH). Tuning width is consistent with a prediction by a cosine tuning function (blue curve), resulting from a linear combination of cone inputs.

The overall difference ΔR_A between a signal region A and the background region B is computed by taking the norm $|\cdot|$ of the contrast between signal and background responses for each channel $i = 1, 2, \ldots, N$:

$$\Delta R_A = \begin{vmatrix} c(R_{A,1}, R_{B,1}) \\ c(R_{A,2}, R_{B,2}) \\ \vdots \\ c(R_{A,N}, R_{B,N}) \end{vmatrix}.$$

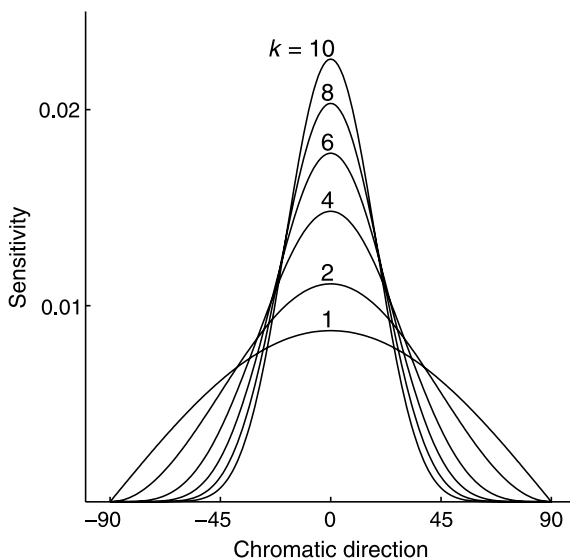
Figure 20. Sensitivity profiles of the chromatic mechanisms for different values of the exponential k.
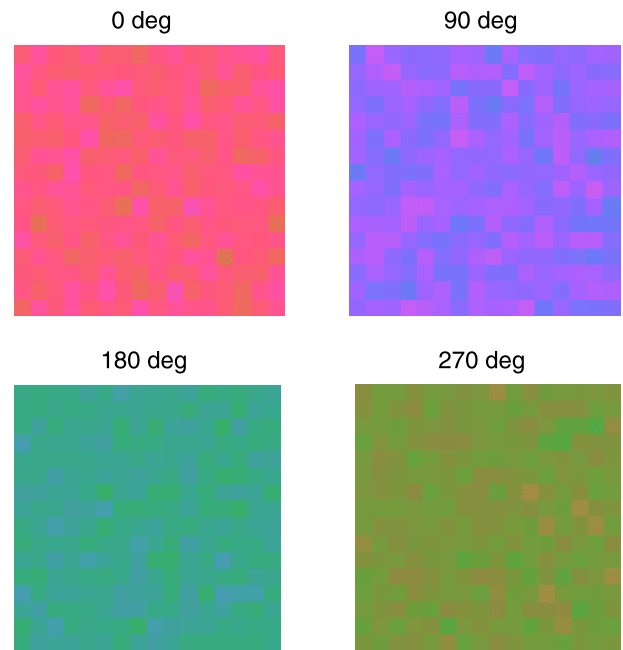

Figure 21. Visualization of the peak sensitivities for a model with $N = 4$ mechanisms. Each panel shows how the peak sensitivities vary across stimulus positions.

We used the Michelson contrast to compute the contrast function c, which is defined as follows:

$$c(x, y) = \frac{x - y}{x + y}.$$

For the norm, we used the standard vector norm (L2 norm, Euclidean distance), which approximates probability summation across channels (Goda & Fujii, 2001; Wilson & Gelb, 1984). The model incorporates no specific interaction between mechanisms other than the pooling of all channels when computing the norm.

Two ΔR values were computed for two putative signal regions A_h and A_v to test for either horizontal or vertical signal orientation (Figure 22). The larger of the two ΔR values then determined the orientation as estimated by the model.

In the simulations, for each stimulus as specified by the signal direction, noise direction, and noise contrast, ΔR values were computed for 1,000 noisy variations of the stimulus. Noise contrast varied in a fixed range. Psychometric functions were then fitted to the model responses for the different noise contrasts to determine the threshold for the particular combination of signal and noise direction. The whole simulation was carried out for two types of noise: one- and two-sided noises.

The fitting of a psychometric function to model responses for different noise contrasts differed from the method used by Goda and Fujii (2001), who employed a single ΔR value as argument of an empirically given psychometric function to directly determine percentage correct. Our simulations need a large number of presentations for each stimulus
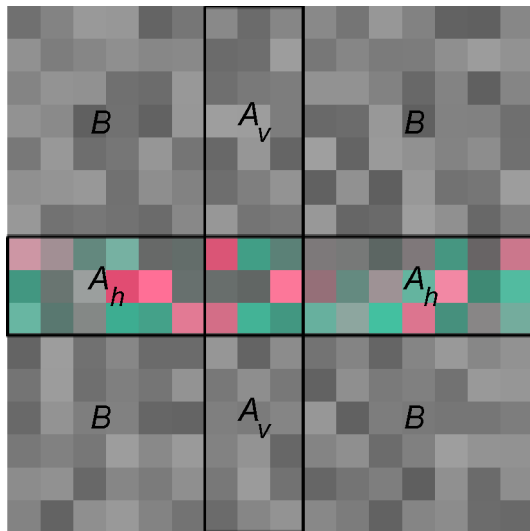
Figure 22. Partitioning of a sample input stimulus into background B and two putative signal regions A_h and A_v. In this example, the ΔR value for A_h would be much larger than the ΔR value for A_v and the model would correctly detect the horizontal signal.

condition but have the advantage of determining the model estimates of threshold values independent of any empirically derived psychometric function.

As stated above, the number N of the detection mechanisms and their tuning width k are basic model parameters. Three models are of particular interest: (1) a basic quasi-linear model with four broadly tuned mechanisms at the cardinal directions ($N = 4$, $k = 1$); (2) a model with multiple narrowly tuned mechanisms with a tuning width similar to the experimentally observed tuning for one-sided noise ($N = 16$, $k = 10$); and (3) a model with multiple broadly tuned mechanisms ($N = 16$, $k = 1$). Simulation results for these three model types are presented in the following.

Simulation results

In a first experiment, we verified that the model faithfully replicates the basic properties of noise masking. In particular, we verified that the model shows a linear increase in threshold with noise contrast when the noise is modulated along the same direction, as well as virtually no increase in threshold when the noise is modulated along directions orthogonal to the signal.

Having verified the basic properties of noise masking, we then investigated the model responses when probed with the masking stimuli used in our experiments, having either one-sided or two-sided noise.

One-sided noise

In a first set of simulations, we used one-sided noise and investigated the model responses for the three different parameter sets. For each parameter set, four signal directions

of 0, 45, 90, and 135 deg were tested, varying along the cardinal directions and along intermediate directions. Noise directions were sampled at 5-deg intervals. Simulations were carried out for different parameter sets. Of particular interest is a basic quasi-linear model with broadly tuned mechanisms along the cardinal directions ($N = 4$, $k = 1$) and models with multiple mechanisms, either narrowly tuned ($N = 16$, $k = 10$) or broadly tuned ($N = 16$, $k = 1$).

Simulations of the model responses for these three parameter sets are shown in Figure 23. For each model, three graphs are shown, namely: model responses for a signal modulated along the cardinal direction (0 deg), model responses for a signal modulated along an intermediate direction (45 deg), and the mean tuning curves averaged across all four signal directions. As a basic result, all models show the highest threshold when noise and signal are modulated along the same direction in color space. The individual shapes of the tuning curves, however, critically depend on the number and tuning width of the mechanisms.

The quasi-linear model ($N = 4$, $k = 1$) failed to reproduce the experimentally observed tuning curves. The model tuning curves differed considerably depending on the direction of the signal color, in contrast to the empirical findings. When the signal was modulated along a cardinal direction of 0 deg (Figure 23, first row, first graph), the model showed a broad tuning consistent with the tuning of the underlying sensitivity function. In this case, no narrow tuning due to off-axis looking occurred because the other channels were centered at directions (of 90 and 270 deg) orthogonal to the signal and received virtually no signal input. A fundamentally different tuning curve resulted when the signal was modulated along an intermediate direction of 45 deg (Figure 23, first row, second graph). In this case, off-axis looking occurred and resulted in a narrow tuning: The four detection mechanisms of the model are located with an offset of 45 deg relative to the signal direction, and those mechanisms least affected by the noise along one direction can contribute to the detection of the signal. However, these mechanisms cannot distinguish between noise along the signal direction (45 deg) and noise along an orthogonal direction (135 deg), both having the same strength when projected to the cardinal mechanisms at 0, 90, 180, and 270 deg. Therefore, noise modulated at parallel or orthogonal directions has essentially the same effect, as revealed by the double lobes of simulated thresholds along the positive and negative diagonal. The small deviations in the model both from a perfectly broad linear tuning for the 0-deg signal and a perfectly symmetrical narrow tuning for the 45-deg signal are due to the random variations of the center of the mechanisms. Overall, the results suggest that more than four mechanisms are needed to account for the empirical data.

The model with multiple narrowly tuned mechanisms ($N = 16$, $k = 10$) resulted in tuning curves narrower than those found experimentally. Finally, the models with multiple linearly tuned mechanisms ($N = 16$, $k = 1$) gave the best fits to the data. We also simulated a model with a smaller number
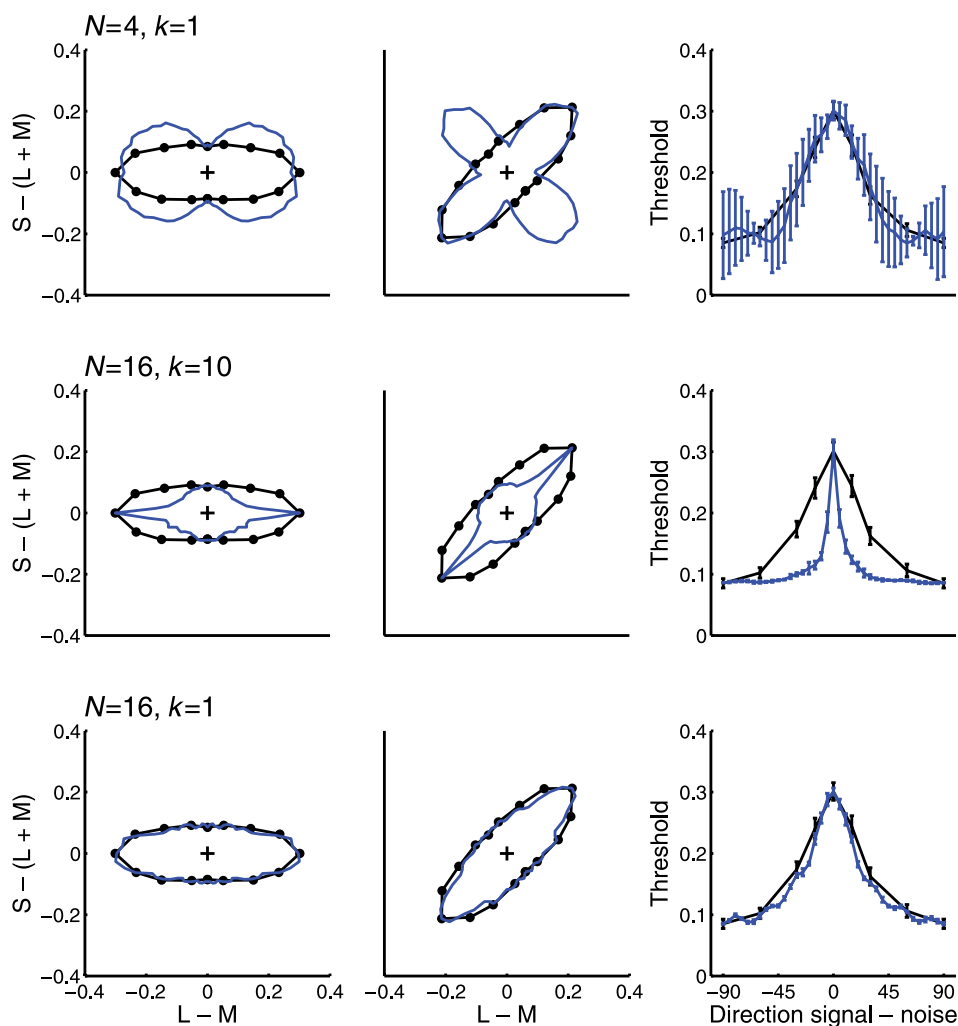
Figure 23. Simulation of model responses using one-sided noise. Simulated curves are shown in blue and empirical data are shown in black for comparison. Columns, from left to right, show the tuning curves for a signal at 0 and 45 deg and the mean tuning curve for four signals at 0, 45, 90, and 135 deg. Each row shows simulation results obtained for a different combination of model parameters N and k, namely, $N = 16$, $k = 1$ (quasi-linear model); $N = 16$, $k = 10$ (multiple narrowly tuned mechanisms); and $N = 16$, $k = 1$ (multiple broadly tuned mechanisms). Error bars denote standard error. Best fits are obtained with multiple broadly tuned mechanisms.

of linearly tuned mechanisms ($N = 8$, $k = 1$). Accuracy of the fit increased with increasing number of mechanisms. Interestingly, the simulations showed that narrow tuning can be produced by multiple broadly tuned mechanisms. Again, the simulated responses were not perfectly symmetric due to the random variation of the peak sensitivities.

Two-sided noise

In a second set of simulations, we investigated the model responses using two-sided noise. All model parameters are identical to the parameters for the one-sided noise. Simulation results are shown in Figure 24.

For two-sided noise, the overall pattern of results closely resembled the pattern obtained for one-sided noise. Again, threshold was maximal when signal and noise directions coincided.

For the quasi-linear cardinal model ($N = 4$, $k = 1$), tuning curves differed for signals modulated along the cardinal as compared with intermediate, noncardinal directions, in contrast to the empirical findings. Although a reasonable fit was obtained for signals modulated along the cardinal directions, tuning curves for signals modulated along intermediate directions were narrower than those observed experimentally. This narrower tuning may be due to some sort of residual off-axes looking, which is possible even in two-sided noise when in the random noise patterns, occasionally, noise in one direction is stronger compared with the other direction. The difference between cardinal and noncardinal directions resulted in the large error bars for the mean responses, in contrast to the empirical data.

The model with multiple narrowly tuned mechanisms ($N = 16$, $k = 10$) completely failed to account for the data.
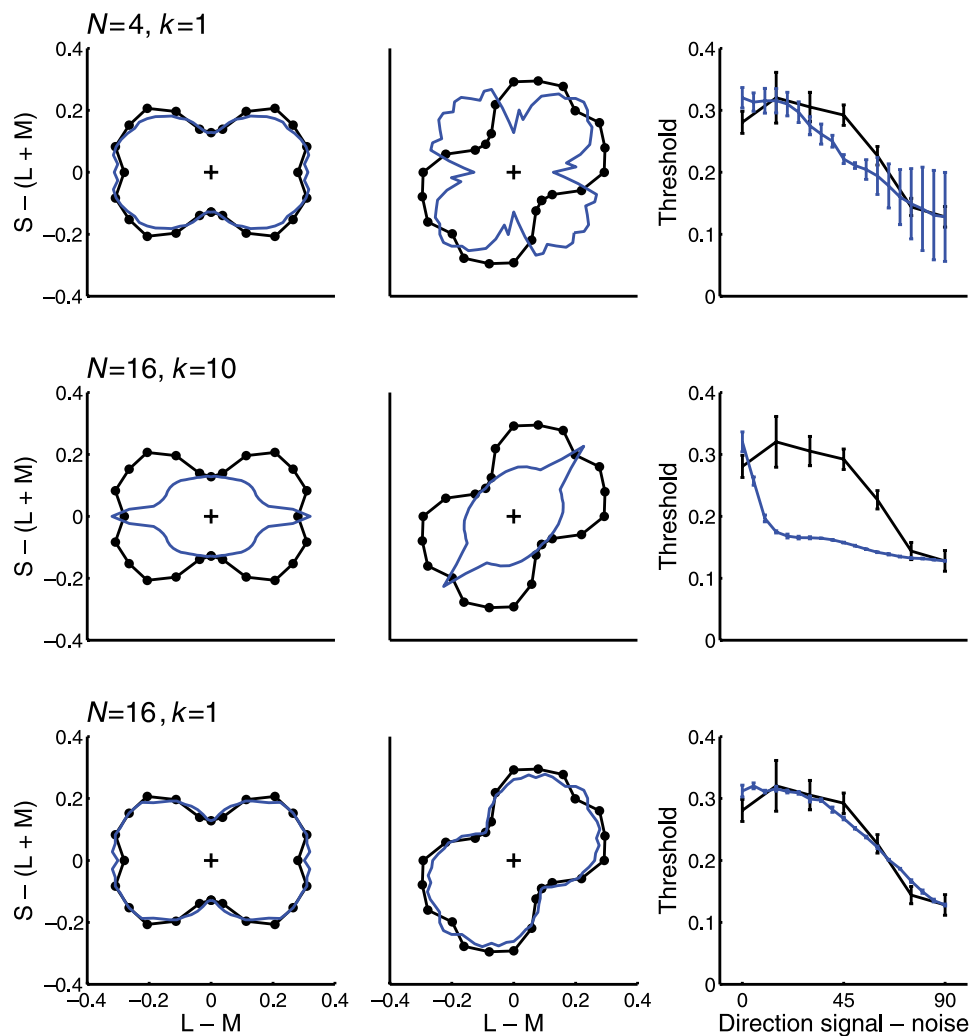
Figure 24. Simulation of model responses using two-sided noise. Simulated curves are shown in blue and empirical data are shown in black for comparison. Columns, from left to right, show the tuning curves for a signal at 0 and 45 deg and the mean tuning curve for four signals at 0, 45, 90, and 135 deg. Each row shows simulation results obtained for a different combination of model parameters N and k, namely, N = 16, k = 1 (quasi-linear model); N = 16, k = 10 (multiple narrowly tuned mechanisms); and N = 16, k = 1 (multiple broadly tuned mechanisms). Error bars denote standard error. As for the one-sided noise, best fits are obtained with multiple broadly tuned mechanisms.

Simulated tuning curves were much narrower than found experimentally.

As for one-sided noise, the model with multiple linearly tuned mechanisms (N = 16, k = 1) closely fit the empirical data.

Overall, the simulation results show that a single detection mechanism can result in different tuning widths, depending on the noise pattern. In particular, the model simulations show that a model with multiple broadly tuned mechanisms can account for the experimentally observed tuning curves, both for one- and two-sided noises. Other model variants, such as a quasi-linear model or a model with multiple narrowly tuned channels, failed to reproduce the empirical findings. A quasi-linear model with four linear mechanisms showed a large variability in tuning curves depending on the signal azimuth, contrary to the empirical data. Models with narrow tuning curves consistently showed narrower than linear tuning for the two-sided noise stimulus, in contrast to the empirical data.

The simulation results thus show that, depending on the stimulus noise, multiple linear mechanisms can result in narrow or broad tuning curves for signals modulated along either cardinal or noncardinal directions, in accordance with the psychophysical observations.

Discussion

In this study, we investigated the number and chromatic properties of mechanisms involved in image segmentation. We used a masking paradigm to study the properties of chromatic signal detection in the isoluminant and the L − M

luminance plane of DKL color space. Two noise patterns were employed, where noise was modulated either along one direction in color space (one-side noise) or along two directions symmetrically spaced around the signal direction (two-sided noise). Two main findings were consistent, independent of the different color planes or the noise pattern used: First, signal masking was strongest when signal and noise were modulated along the same direction and monotonically decreased with increasing difference between signal and noise direction. Second, no difference was found for signals presented along the cardinal directions versus intermediate, noncardinal directions in DKL color space. However, depending on the noise used, the width of chromatic tuning significantly differed: For one-sided noise, narrowly tuned curves were obtained, whereas for two-sided noise, broad tuning was found, consistent with a linear combination of cone inputs. Next, we used a chromatic detection model to further study the number and nature of the underlying chromatic mechanisms. The simulations show that the tuning curves for both kinds of noise can be a generated by multiple broadly tuned mechanisms.

Chromatic detection model

The aim of the simulations using the chromatic detection model was to clarify how vastly different tuning curves observed for different types of noise can be accounted for by the same underlying mechanisms. We demonstrated that indeed a model with multiple broadly tuned mechanisms is in good accordance with the data.

The present model does not account for the differences in detection threshold *in the absence of noise* generally found along the cardinal axes. This would require the inclusion of internal noise, which is not constrained by our data. Furthermore, because a higher sensitivity affects both the noise and the signal in the same way, adding internal noise may not change the noise-masking predictions fundamentally.

The present model does not account for the small dip when signal and noise coincide, which results in the bow-tie shape in some of the empirically found tuning curves. In preliminary simulation studies, we found that a specific decrease in the variability of the mechanisms along the signal direction results in the observed dip. Other factors that might contribute to this dip are an unequal distribution of the detection mechanisms along the chromatic directions and the variability of the tuning widths found in the V1 and V2 neurons. A final conclusive explanation of this small effect is beyond the scope of the present model and article.

The present model does not aim to account for detection thresholds in the absence of noise or to fit every detail in the empirical data. Instead, we present a basic minimal model with just two fundamental parameters (N and k) and show how a single parameter set with multiple broadly tuned mechanisms accounts for two fundamentally different widths of tuning curves resulting from two noise types. Empirical data from psychophysics (e.g., detection thresholds in the absence of

noise) and physiology (e.g., variation of tuning width, distribution of preferred chromatic direction, adaptation) offer promising possibilities to extend the model in various ways.

Comparison with other studies

A number of studies have investigated chromatic signal detection. One of the first studies that used a noise-masking paradigm was the study by Gegenfurtner and Kiper (1992). Using a Gabor pattern as signal embedded in spatiotemporal chromatic noise, they found multiple narrowly tuned mechanisms.

Li and Lennie (1997) determined the chromatic mechanisms involved in texture segmentation. Observers had to detect a target, made of random noise squares along a particular color direction, amid a background noise made of squares whose color was chosen along the same or another line in color space. They found evidence mainly for additional noncardinal mechanisms in the isoluminant plane. Evidence for cardinal mechanisms was found only when stimuli were modulated in luminance and in one of the cardinal directions. They also found large differences between their observers, especially with respect to the bandwidth of chromatic tuning. This might be due to their rather coarse sampling of color space. Furthermore, their stimuli were notably different from those used by Gegenfurtner and Kiper (1992). In particular, the signal distributions were not only symmetrically modulated around the origin but also contained a shift in color space.

The stimuli used by Sankeralli and Mullen (1997) were identical to the ones used by Gegenfurtner and Kiper (1992), with the exception that static noise was used instead of dynamic noise. Sankeralli and Mullen found a wider bandwidth of chromatic tuning. When using signals in intermediate directions of color space, they observed no masking for noise along orthogonal directions, which is clear evidence for mechanisms tuned to these intermediate directions.

Giulianini and Eskew (1998) measured thresholds for detecting Gaussian and Gabor signals in noise made of rings or lines. Signal and noise were modulated independently along various directions of color space. Their results argue for only three mechanisms for chromatic detection. These mechanisms are strictly linear; that is, they do not exhibit a narrow tuning in color space. The reason for the discrepancy in their results from those of Gegenfurtner and Kiper (1992) is unclear.

More recently, Eskew, Newton, and Giulianini (2001) studied detection and threshold-level discrimination of Gabor patches under conditions of noise masking, attempting to isolate higher order mechanisms. Neither the detection nor the discrimination procedure revealed any evidence of additional mechanisms besides the cardinal ones.

Stromeyer et al. (1999) used sine waves for their signals and noise maskers. They found evidence for intermediate higher level chromatic mechanisms whenever there were phase offsets between signals and noise. They argue that

the narrow and specific tuning observed by Gegenfurtner and Kiper (1992) might be due to the spatial differences in signals and noise maskers.

D'Zmura and Knoblauch (1998) used Gaussian blobs as their signals and noise stimuli. The signal was modulated along a certain direction of color space, whereas the noise was chosen from within a sector of color space with varying width. They found that contrast thresholds were largest when signals and noise were modulated along the same directions of color space, even for noncardinal, intermediate directions. This argues for many chromatic detection mechanisms. However, the magnitude of noise masking did not depend on the widths of the noise sectors. This argues for linearly tuned mechanisms. Consequently, the results of D'Zmura and Knoblauch suggest multiple broadly tuned mechanisms, as in the present study. Nonlinear narrow tuning observed in some experiments is due to off-axis looking.

Goda and Fujii (2001) investigated the discriminability of multicolored textures made of squares whose color was drawn from different distributions in DKL color space. The amplitude of the color distributions was modulated sinusoidally at various chromatic frequencies. Their results were consistent with multiple sharper than linear mechanisms with an HWHH of 40 deg. The difference in results may be due to the large size of the stimulus of 8×8 deg and the specific properties of stimuli having sinusoidally modulated contrast amplitudes.

More recently, Lindsey and Brown (2004) investigated the masking of grating detection in the isoluminant plane of DKL color space. Using two-sided noise, they found evidence for off-axis looking. Similar to the present study, the data were well accounted for by a model of multiple broadly tuned mechanisms. In their study, detection thresholds were measured only at two intermediate directions (135 and 160 deg) in the isoluminant plane of DKL color and no alternative model was tested. The present study is a more in-depth investigation of the number and nature of higher order mechanisms.

Although stimuli, results, and interpretation vary between groups, the existence of multiple mechanisms beyond the four tuned to the cardinal directions of color space is supported by a large amount of empirical data. Physiological findings suggest a hierarchy of processing stages, each characterized by tuning width varying in a certain range around the linear tuning with an HWHH of 60 deg. A number of psychophysical studies suggest that multiple broadly tuned mechanisms play an important role in chromatic signal discrimination.

Conclusions

We used a noise-masking paradigm to investigate the chromatic detection in two planes of DKL color space, the isoluminant plane and the L − M luminance plane. Two noise patterns of either one-sided or two-sided noise were employed. The experimentally observed tuning curves critically depend on the noise pattern used. Narrow tuning is observed for one-sided noise, whereas broad tuning is observed for two-sided noise. The psychophysical experiments are accompanied by a model study, showing that the observed data can be accounted for by the same underlying processing based on multiple broadly tuned mechanisms.

Furthermore, no difference was found between signals modulated along the cardinal and those modulated along intermediate directions. All results hold true for the isoluminant and the L − M luminance plane.

Overall, the results suggest that higher order cortical mechanisms with multiple broadly tuned mechanisms are involved in the segmentation of chromatic surfaces.

Acknowledgments

Commercial relationships: none.
Corresponding authors: Thorsten Hansen and Karl R. Gegenfurtner.
Email: Thorsten.Hansen@psychol.uni-giessen.de and Karl.R.Gegenfurtner@psychol.uni-giessen.de.
Address: Justus-Liebig-University Giessen, Department of Psychology, Otto-Behaghel-Str. 10F, D-35394 Giessen, Germany.

References

Brainard, D. H. (1989). Calibration of a computer controlled color monitor. *Color Research & Application, 14,* 23–34.

Clifford, C. W., Spehar, B., Solomon, S. G., Martin, P. R., & Zaidi, Q. (2003). Interactions between color and luminance in the perception of orientation. *Journal of Vision, 3*(2), 106–115, http://journalofvision.org/3/2/1/, doi:10.1167/3.2.1. [PubMed] [Article]

Derrington, A. M., Krauskopf, J., & Lennie, P. (1984). Chromatic mechanisms in the lateral geniculate nucleus of macaque. *The Journal of Physiology, 357*, 241–265. [PubMed]

De Valois, R. L., & De Valois, K. K. (1993). A multi-stage color model. *Vision Research, 33,* 1053–1065. [PubMed]

D'Zmura, M. (1991). Color in visual search. *Vision Research, 31,* 951–966. [PubMed]

D'Zmura, M., & Knoblauch, K. (1998). Spectral bandwidths for the detection of color. *Vision Research, 38,* 3117–3128. [PubMed]

D'Zmura, M., & Lennie, P. (1986). Mechanisms of color constancy. *Journal of the Optical Society of America A, Optics and Image Science, 3,* 1662–1672. [PubMed]

Eskew, R. T., Jr., Newton, J. R., & Giulianini, F. (2001). Chromatic detection and discrimination analyzed by a Bayesian classifier. *Vision Research, 41,* 893–909. [PubMed]

Gegenfurtner, K. R. (2000). Higher level chromatic mechanisms for image segmentation. [Abstract] *Investigative Ophthalmology & Visual Science, 41,* S742.

Gegenfurtner, K. R. (2003). Cortical mechanisms of colour vision. *Nature Reviews: Neuroscience, 4,* 563–572. [PubMed]

Gegenfurtner, K. R., & Kiper, D. C. (1992). Contrast detection in luminance and chromatic noise. *Journal of the Optical Society of America A, Optics and Image Science, 9,* 1880–1888. [PubMed]

Gegenfurtner, K. R., Kiper, D. C., & Levitt, J. B. (1997). Functional properties of neurons in macaque area V3. *Journal of Neurophysiology, 77,* 1906–1923. [PubMed] [Article]

Giulianini, F., & Eskew, R. T., Jr. (1998). Chromatic masking in the (ΔL/L, ΔM/M) plane of cone-contrast space reveals only two detection mechanisms. *Vision Research, 38,* 3913–3926. [PubMed]

Goda, N., & Fujii, M. (2001). Sensitivity to modulation of color distribution in multicolored textures. *Vision Research, 41,* 2475–2485. [PubMed]

Hansen, T., & Gegenfurtner, K. R. (2005). *Modeling chromatic signal detection using multiple broadly tuned mechanisms*. Proceedings of the 9th International Conference on Cognitive and Neural Systems (ICCNS 2005) (p. 12). Boston: Boston University.

Hering, E. (1878). *Zur Lehre vom Lichtsinn*. Wien, Austria: Gerold.

Hurvich, L. M., & Jameson, D. (1957). An opponent-process theory of color vision. *Psychological Review, 64,* 384–404. [PubMed]

Irtel, H. (1992). Computing data for color vision modeling. *Behavior Research Methods, Instruments, & Computers, 24,* 387–401.

Judd, D. B. (1951). *Report of US Secretariat Committee on Colorimetry and Artificial Daylight*. Proceedings of the Twelfth Session of the CIE, Stockholm, Sweden, p. 11. Bureau Central de la CIE, Paris, France.

Kaplan, E., Lee, B. B., & Shapley, R. (1990). New views of primate retinal function. In N. Osborne & G. Chader (Eds.), *Progress in retinal research* (Vol. 9, pp. 273–336). Oxford: Pergamon Press.

Kiper, D. C., Fenstemaker, S. B., & Gegenfurtner, K. R. (1997). Chromatic properties of neurons in macaque area V2. *Visual Neuroscience, 14,* 1061–1072. [PubMed]

Knoblauch, K., & D'Zmura, M. (2001). Lights and neural responses do not depend on choice of color space [Reply to letter to editor by M. J. Sankeralli and K. T. Mullen published in *Vision Research, 41,* 53–55]. *Vision Research, 41*(13), 1683–1684. [PubMed]

Komatsu, H. (1998). Mechanisms of central color vision. *Current Opinion in Neurobiology, 8,* 503–508. [PubMed]

Komatsu, H., Ideura, Y., Kaji, S., & Yamane, S. (1992). Color selectivity of neurons in the inferior temporal cortex of the awake macaque monkey. *The Journal of Neuroscience, 12,* 408–424. [PubMed] [Article]

Krauskopf, J., Williams, D. R., & Heeley, D. W. (1982). Cardinal directions of color space. *Vision Research, 22,* 1123–1131. [PubMed]

Krauskopf, J., Williams, D. R., Mandler, M. B., & Brown, A. M. (1986). Higher order color mechanisms. *Vision Research, 26,* 23–32. [PubMed]

Krauskopf, J., Wu, H. J., & Farell, B. (1996). Coherence, cardinal directions and higher-order mechanisms. *Vision Research, 36,* 1235–1245. [PubMed]

Legge, G. E., Kersten, D., & Burgess, A. E. (1987). Contrast discrimination in noise. *Journal of the Optical Society of America A, Optics and Image Science, 4,* 391–404. [PubMed]

Lennie, P., Krauskopf, J., & Sclar, G. (1990). Chromatic mechanisms in striate cortex of macaque. *The Journal of Neuroscience, 10,* 649–669. [PubMed] [Article]

Levitt, H. (1971). Transformed up-down method in psychoacoustics. *The Journal of the Acoustical Society of America, 49,* 467–477. [PubMed]

Li, A., & Lennie, P. (1997). Mechanisms underlying segmentation of colored textures. *Vision Research, 37,* 83–97. [PubMed]

Lindsey, D. T., & Brown, A. M. (2004). Masking of grating detection in the isoluminant plane of DKL color space. *Visual Neuroscience, 21,* 269–273. [PubMed]

MacLeod, D. I., & Boynton, R. M. (1979). Chromaticity diagram showing cone excitation by stimuli of equal luminance. *Journal of the Optical Society of America, 69,* 1183–1186. [PubMed]

Pelli, D. (1981). *The effect of visual noise*. PhD dissertation. Cambridge, UK: Cambridge University.

Pugh, E. N., Jr., & Mollon, J. D. (1979). A theory of the Π_1 and Π_3 color mechanisms of Stiles. *Vision Research, 19,* 293–312. [PubMed]

Sankeralli, M. J., & Mullen, K. T. (1997). Postreceptoral chromatic detection mechanisms revealed by noise masking in three-dimensional cone contrast space. *Journal of the Optical Society of America A, Optics, Image Science, and Vision, 14,* 2633–2646. [PubMed]

Smith, V. C., & Pokorny, J. (1975). Spectral sensitivity of the foveal cone photopigments between 400 and 500 nm. *Vision Research, 15,* 161–171. [PubMed]

Stromeyer, C. F., III., Thabet, R., Chaparro, A., & Kronauer, R. E. (1999). Spatial masking does not reveal mechanisms selective to combined luminance and red-green color. *Vision Research, 39,* 2099–2112. [PubMed]

von Helmholtz, H. L. F. (1924). *Helmholtz' treatise on physiological optics* (J. P. C. Southall, Trans.). New York: Optical Society of America. (Original work "Handbuch der physiologischen Optik" published 1867. Leipzig, Germany: Voss.)

Wachtler, T., Sejnowski, T. J., & Albright, T. D. (2003). Representation of color stimuli in awake macaque primary visual cortex. *Neuron, 37*(4), 681–691. [PubMed]

Wandell, B. A., & Pugh, E. N., Jr. (1980). Detection of long-duration, long-wavelength incremental flashes by a chromatically coded pathway. *Vision Research, 20,* 625–636. [PubMed]

Watamaniuk, S. N., Sekuler, R., & Williams, D. W. (1989). Direction perception in complex dynamic displays: The integration of direction information. *Vision Research, 29,* 47–59. [PubMed]

Webster, M. A., & Mollon, J. D. (1991). Changes in colour appearance following post-receptoral adaptation. *Nature, 349,* 235–238. [PubMed]

Webster, M. A., & Mollon, J. D. (1994). The influence of contrast adaptation on color appearance. *Vision Research, 34,* 1993–2020. [PubMed]

Wichmann, F. A., & Hill, N. J. (2001). The psychometric function: I. Fitting, sampling and goodness of fit. *Perception & Psychophysics, 63,* 1293–1313. [PubMed]

Wilson, H. R., & Gelb, D. J. (1984). Modified line-element theory for spatial-frequency and width discrimination. *Journal of the Optical Society of America A, Optics and Image Science, 1,* 124–131. [PubMed]

Wyszecki, G., & Stiles, W. S. (1982). *Color science concepts and methods, quantitative data and formulae.* New York: Wiley.

Zaidi, Q., & Shapiro, A. G. (1993). Adaptive orthogonalization of opponent-color signals. *Biological Cybernetics, 69,* 415–428. [PubMed]